

Interplay and specific features of radiation mechanisms of electrons and positrons in crystalline undulators

Alexander V. Pavlov,^{1,2,*} Andrei V. Korol,^{2,3,†} Vadim K. Ivanov,¹ and Andrey V. Solov'yov³

¹*Peter the Great St. Petersburg Polytechnic University,
Polytechnicheskaya 29, 195251 St. Petersburg Russia*

²*St. Petersburg State Maritime University,
Leninsky ave. 101, 198262 St. Petersburg Russia*

³*MBN Research Center, Altenhöferallee 3, 60438 Frankfurt am Main Germany*

We predict peculiar changes in spectral distributions of radiation emitted by ultra-relativistic positrons and electrons in periodically bent crystals with variation of the bending amplitude. It is shown that the changes, being sensitive to the projectile energy, manifest themselves differently for negatively and positively charged projectiles. We demonstrate that the features observed are due to the interplay of different radiation mechanisms occurring in periodically bent crystals. The observations are important for design, practical realization and channeling experiments with periodically bent crystals as the key element of the novel light sources. The analysis presented is based on the grounds of accurate numerical simulations of the channeling process.

PACS numbers: 61.85.+p, 41.60.-m, 41.75.Ht, 02.70.Uu, 07.85.Fv

For several decades, propagation of relativistic charged particles in oriented crystals remains in focus of challenging research. As predicted by Lindhard [1], the projectiles penetrate large distances moving along a crystallographic direction. The channeling phenomenon has been receiving a significant interest, both with respect to a fundamental theory and the experiments. In straight crystals, the intensity of radiation emitted by channeling particles (the channeling radiation, ChR [2]) exceeds by orders of magnitude the background bremsstrahlung (BrS) radiation in the amorphous medium. In addition to ChR, in crystals bent with a uniform curvature $1/R$ the radiation acquires features of the synchrotron radiation (SR) [3–5].

Another type of radiation appears in a *crystalline undulator* (CU) in which a beam of ultra-relativistic electrons or positrons undergoes planar channeling in a periodically bent crystal (PBC) [6, 7]. The periodic bending of the planes gives rise to the spontaneous undulator-type CU radiation (CUR) which can be generated in the range of wavelengths λ from 0.1 down to 10^{-6} Å. Its intensity and characteristic frequencies can be varied by changing the beam energy, the

parameters of bending and the type of a crystal. The CUR peak brilliance can be considered at the level of 10^{25} photons/s mrad² mm² 0.1%BW in the photon energy range 0.1 – 10 MeV [8] which cannot be reached in modern undulators based on magnets [9]. Present technologies are nearly sufficient to meet the conditions needed to achieve the emission stimulation in a CU [8]. The scheme for practical realization of a CU laser was patented [10]. This device will be capable of emitting FEL-type radiation with $\lambda = 10^{-3} - 10^{-1}$ Å, i.e. orders of magnitude shorter than in the current XFEL facilities [11–15]). Light source in the hard-X and gamma ray energy range can open new possibilities for various experiments and applications [16–19]. This is a very ambitious goal, which imposes further refinement of the existing apparatus, new experimental approaches and technologies as well as development of state-of-the-art theoretical and computational methods. However, the efforts in this direction will certainly make this field of endeavour even more fascinating.

The feasibility for the CU scheme was predicted and verified theoretically only very recently [6, 7, 20–22]. In these papers, as well

as in the subsequent publications (see Ref. [8] for the latest review), essential conditions and limitations which must be met to make possible the observation of the effect were formulated. These papers triggered a sharp increase in publications on the subject worldwide, so that one can state that this topic represents a new, rich and very promising field of research.

In recent years, electron channeling and radiation in bent crystals have been extensively studied both theoretically and experimentally [5, 23–39]. A set of experiments have been performed aiming at detecting the CUR. The most recent ones include experiments at the MAINZER MICROTRON (MAMI) [23, 40], CERN [41] and SLAC [42]. So far, these attempts have not been entirely conclusive most probably due to a not sufficient quality of the probed periodically bent (PB) crystalline structures [43].

In this Letter, we predict peculiar changes in the emission spectra with variation of the amplitude a of periodic bending. These modifications are sensitive to the projectile energy ε and manifest themselves differently for negative and positive projectiles. We demonstrate that the features observed are due to the interplay of different radiation mechanisms occurring in periodically bent crystals, namely, the ChR, the CUR, the SR and the coherent BrS.

Numerical modeling of the channeling phenomena was performed by means of the multi-purpose computer package MBN EXPLORER [44, 45]. The channeling module of the package [46] allows for multiscale all-atom molecular dynamics simulations of the ultra-relativistic projectiles propagation and radiation in various environments including the crystalline one. The code was benchmarked for various ultra-relativistic projectiles channeling [8, 23, 36, 46–48]. The atomistic approach implemented in MBN Explorer, combined with modern numerical algorithms, advanced computational facilities and computing technologies makes the predictive power of the software comparable or maybe even higher than the accuracy achievable experimentally. Thus, the computational mod-

eling becomes a tool that could substitute (or become an alternative to) expensive laboratory experiments, and thus reduce the experimental and technological costs.

In line with the experimental conditions for electrons at MAMI [23] and with those potentially achievable for positrons [49], we simulated the channeling of $\varepsilon = 270 - 855$ MeV electrons and positrons in $L = 20$ μm thick straight and PB diamond(110) crystals. The harmonic bending shape $S(z) = a \cos(2\pi z/\lambda_u)$ was assumed with the coordinate z measured along the incident beam direction. The bending period λ_u was fixed at the value of 5 μm , the range of bending amplitude includes the values $a = 1.2, 2.5, 4.0$ \AA . The values of $\varepsilon, L, \lambda_u$ and a quoted above correspond to those used in recent experiments at MAMI [50].

For each set of the parameters, $N = 6000$ trajectories were simulated. Due to randomness in sampling the incoming projectiles and in positions of the lattice atoms due to the thermal fluctuations each simulated trajectory corresponds to a unique crystalline environment [46]. Thus, all simulated trajectories are statistically independent and can be analyzed to quantify the channeling process as well as the emitted radiation. For each trajectory spectral distribution of the emitted radiation was calculated within the cone $\theta \leq \theta_0 = 0.24$ mrad. The resulting spectrum was obtained by averaging over *all* trajectories, and thus it accounts for contributions of the channeling segments as well as of those corresponding the non-channeling regime. Figure 1 presents the calculated spectral distributions for 855 MeV projectiles.

Figure 1(a) serves reference purposes and illustrates well-established features of the emission spectra in straight crystals (see, e.g., Ref. [51]). For both electrons and positrons the spectra are dominated by peaks of ChR, the intensities of which by far exceed that of BrS in the amorphous medium. Different character of channeling oscillations by positrons and electrons result in differences in the peak profiles. For positrons, nearly perfect harmonic

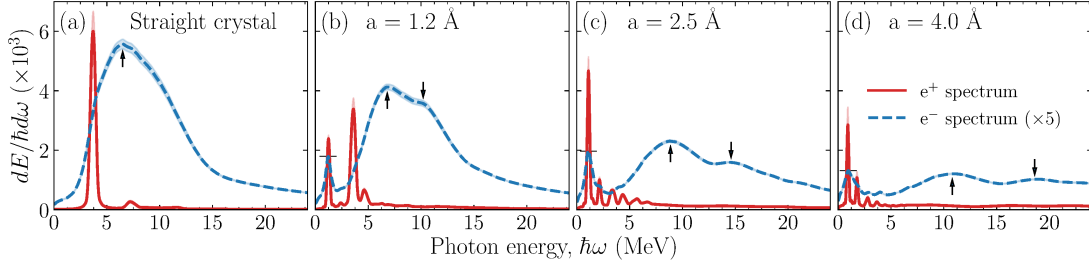


FIG. 1. Spectral distributions of radiation by 855 MeV electrons and positrons for the straight (a) and PB diamond (110) crystal for different bending amplitudes as indicated in (b-d). The electron spectra are multiplied by factor 5. The upward arrows indicate the maxima of ChR for electrons, the downward arrows show the positions of the additional maxima appearing in the PBCs. Grey shading indicates statistical errors due to the finite number of simulated trajectories. For the sake of comparison, we mention that the intensity of the background radiation (not shown in the figure) due to the incoherent BrS, estimated within the Bethe-Heitler approximation is 0.025 (in the units 10^{-3} used in the figure).

channeling oscillations give rise to a narrow, undulator-type peak at $\hbar\omega \approx 3.6$ MeV. A much less intensive peak at ≈ 7.2 MeV corresponds to the emission in the second harmonics. For electrons, strong anharmonicity of the channeling oscillations results in significant broadening and lowering of the peak (note that the electron spectra in are multiplied by factor five).

In the PBCs, Figs. 1 (b)-(d), the spectra exhibit additional features some of which evolve differently with the increase in a .

(I) First, there are CUR peaks in the low-energy parts of the spectra. The most powerful of these correspond to the emission in the fundamental harmonic of CUR at $\hbar\omega_1 \approx 1$ MeV in both electron ('-') and positron ('+') spectra. To be noted is the non-monotonous dependence of the peak intensities, $I_{\text{CUR}}^{(\pm)}(a)$, on a .

(II) The second feature, concerns a strong suppression of ChR in the positron spectra as a increases. Indeed, for periodic bending with $a = 1.2$ Å the ChR intensity, $I_{\text{ChR}}^{(+)}(a)$, drops by a factor of two as compared to the straight crystal, $a = 0$, whereas for larger bending amplitudes the ChR peak virtually disappears.

(III) Finally, we mention the evolution of the electron ChR spectrum. Its intensity $I_{\text{ChR}}^{(-)}(a)$ does not fall off so dramatically as for positrons.

Next, as a increases the ChR peak (marked with the upward arrow in each graph) becomes more blue-shifted and there appears additional structure (the downward arrows) on the right shoulder of the spectrum.

In what follows, the physical explanation of these novel features is provided.

A particle, channeled in a PBC, experiences two types of quasi-periodic motions: due to the channeling oscillations and because of periodic bending of the crystal planes. To estimate the dependence of ChR and CUR on the bending amplitude a , one notices that intensity I of the radiation emitted by a bunch of particles is proportional to (i) average number $\langle N \rangle$ of particles participating in the motion, (ii) average distance $\langle L \rangle$ covered by a particle, (iii) squared Fourier image of the particle's acceleration, which can be written as $\Omega^4 A^2$ with Ω and A standing for the frequency and the (average) amplitude of the quasi-periodic motion:

$$I \propto \langle N \rangle \langle L \rangle \Omega^4 A^2. \quad (1)$$

This general relation can be applied to both electrons and positrons.

Let us first analyze the case of a positron channeling. In a planar channeling regime, a charged projectile moves along the planar di-

rejection experiencing a collective action of the electrostatic field of the lattice atoms [1]. For a positively charged projectile, the field is repulsive, so that the particle is steered into the inter-atomic region and oscillates (channels) in between two adjacent crystal planes. At some stage, due to the collisions with the crystal constituents, the transverse energy becomes large enough to allow particle to leave the channeling mode, i.e. to dechannel. The opposite process, the re-channeling, is associated with the capture to the channeling mode. In a sufficiently thick crystal, a projectile can experience dechanneling and re-channeling several times in the course of propagation. In this case, the quantity $\langle L \rangle$ should account for the length of all channeling segments in the trajectory. However, for relatively thin crystals, $L \ll L_d$, (where L_d denotes the dechanneling length, i.e. the average length of a channeling segment in a sufficiently thick crystal, e.g., [53]), the re-channeling events are rare. This feature has been revealed also in a series of recent simulations [5, 8, 34, 35, 39]. Using Eq. (1.50) from [53] one estimates L_d for a 855 MeV positron in diamond(110) as ca 500 μm which is much larger than the thickness $L = 20 \mu\text{m}$. In this limit, the quantity $\langle L \rangle$ can be calculated as a mean penetration length L_p of the accepted particles, i.e. those captured into the channeling mode at the crystal entrance. Correspondingly, the quantity $\langle N \rangle$ can be associated with the number of accepted particles, N_{acc} , which is related to the channel acceptance $\mathcal{A} = N_{\text{acc}}/N$ with N being the total number of particles. The acceptance is maximum for a straight crystal, and gradually decreases with increase in the bending curvature $1/R$ due to the action of the centrifugal force [52]. In a PBC, the maximum curvature of the cosine bending profile $1/R_{\text{max}} \approx 4\pi^2 a/\lambda_u^2$ increases with a , leading to the decrease in N_{acc} as well as in the values of L_p .

The second and third columns in Table I summarize the data on $\mathcal{A}(a)$ and $L_p(a)$ obtained via statistical analysis of the simulated trajectories of positrons (the value $a = 0$ stands for

TABLE I. Acceptance \mathcal{A} , penetration depth of accepted particles L_p , mean squared amplitude of channeling oscillations $\langle a_{\text{ch}}^2 \rangle$ (in units of d^2 , $d = 1.26 \text{ \AA}$ stands for the (110) interplanar spacing), and total length of channeling segments L_{tot} for 855 MeV projectiles in 20 μm thick straight ($a = 0$) and PB diamond(110) crystal.

a (\AA)	positrons			electrons		
	\mathcal{A}	L_p (μm)	$\langle a_{\text{ch}}^2 \rangle/d^2$	\mathcal{A}	L_p (μm)	L_{tot} (μm)
0	0.96	19.3 ± 0.1	0.060	0.72	10.9 ± 0.3	11.8 ± 0.3
1.2	0.82	19.0 ± 0.2	0.042	0.48	7.3 ± 0.3	8.0 ± 0.2
2.5	0.60	16.8 ± 0.3	0.033	0.29	5.0 ± 0.3	4.4 ± 0.2
4.0	0.24	15.1 ± 0.6	0.010	0.20	3.5 ± 0.2	2.5 ± 0.1

the straight channel). These data allows one to qualitatively analyze the dependence of the intensity $I_{\text{CUR}}^{(+)}$ of CUR for positrons on a . Using Eq. (1) and taking into account the independence on the amplitude the factor Ω_u^2 is independent on the amplitude, one writes: $I_{\text{CUR}}^{(+)}(a) \propto \mathcal{A}(a)L_p(a)a^2$. Here, the product of a decreasing $\mathcal{A}(a)L_p(a)$ and an increasing a^2 functions of bending amplitude results in the existence of a_{max} which ensures the maximum value of the CUR intensity.

Similar methodology is applicable to analyze the dependence of the ChR intensity $I_{\text{ChR}}^{(+)}$ on a . In this case, assuming the harmonic character of the channeling oscillations, one writes Eq. (1) as follows: $I_{\text{ChR}}^{(+)} \propto \mathcal{A}(a)L_p(a)\langle a_{\text{ch}}^2 \rangle(a)$. Here, $\langle a_{\text{ch}}^2 \rangle(a)$ stands for the mean square amplitude of the channeling oscillations. This quantity is a decreasing function of a . Indeed, as a increases, the centrifugal force, especially in the vicinity of the points of the maximum curvature, drives the projectiles oscillating with large amplitudes away from the channel resulting in a strong quenching of channeling oscillations. The fourth column in Table I provides the data on $\langle a_{\text{ch}}^2 \rangle$. Thus, gradual decrease in all three factors, \mathcal{A} , L_p and $\langle a_{\text{ch}}^2 \rangle$ results in a considerable drop in the intensity of ChR: the value of $I_{\text{ChR}}^{(+)}$ at $a = 4 \text{ \AA}$ is by a factor of 30 less than for the straight channel, which is in accordance with the trend seen in Fig. 1.

To explain the transformations in the emis-

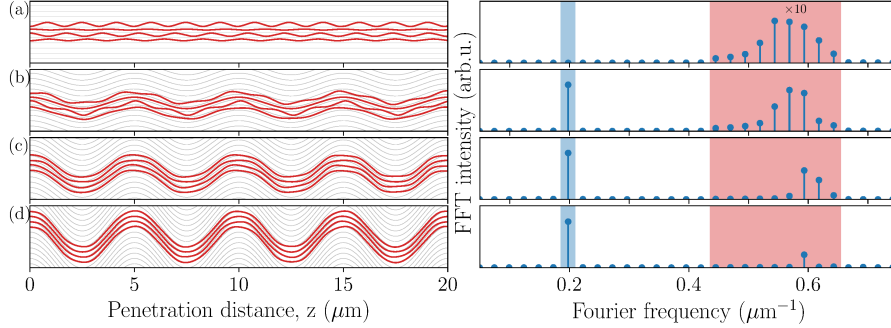


FIG. 2. The 2D projections of several *exemplary* trajectories of the 855 MeV positrons (left) channeled through the whole $L = 20 \mu\text{m}$ thick diamond(110). Thin lines mark the crystalline channels for positrons. Graphs (a)-(d) refer to $a = 0$ (the straight crystal), 1.2, 2.5 and 4.0 Å, correspondingly. The corresponding FFT spectra calculated from *all* channeled trajectories are presented on the right panel. The blue (left) vertical strip marks the Fourier signal due to the periodic bending, the red (right) strip shows the part of the spectrum due to channeling oscillation (note the scaling factor 10).

sion spectra, let us propose an alternative approach based on a quantitative analysis of oscillatory modes of the simulated trajectories by means of the fast Fourier transform (FFT). This approach allows one to visualize the impact of a on the amplitude of channeling oscillations.

Illustrative left panel in Fig. 2 shows several trajectories of positrons which propagate through the whole crystal in the channeling regime. The right panel presents the FFT spectral distributions calculated from all channeling trajectories. In graphs (b)-(d), corresponding to the PBCs, the FFT signals at $f = 0.2 \mu\text{m}^{-1}$ correspond to the motion along the cosine centerline with the period $\lambda_u = 5 \mu\text{m}$. These peaks are normalized via division by a .

By comparing the spectra within the interval $f = 0.45 - 0.65 \mu\text{m}^{-1}$ (indicated in the red shading) for the straight and PBCs one sees the modification of the distribution of channeling oscillations with respect to the amplitude $a_{\text{ch}} \propto \text{FFT}$ and frequency $\Omega_{\text{ch}} \propto f$. In particular, the FFT spectra clearly indicate that with increase in the bending amplitude the ChR intensity decreases significantly.

To conclude the discussion of the positron

case, we remark on the dependence of the profile of the emitted spectrum on the projectile energy. Lower values of ε lead to weakening of the centrifugal force $\varepsilon/R_{\text{max}}$ which, in turn, lessens the suppression of the ChR contribution to the spectrum in a PBC. Figure 3 illustrates the evolution of the emission spectra with ε and a . Left graph corresponds to the straight crystal and thus shows the peaks due to the ChR (note the scaling factor for the $\varepsilon = 270$ and 375 MeV spectra). With increase in a , middle and right graphs, the ChR peak for the 855 MeV projectiles virtually disappears, whereas for lower ε it is still well pronounced.

Let us now turn to the emission spectra due to electrons, see Fig. 1. In contrast to the positron case, the dechanneling length L_d of the 855 MeV electrons in straight diamond(110) is less than the crystal thickness $L = 20 \mu\text{m}$. Our analysis of the trajectories simulated in a much thicker crystal ($140 \mu\text{m}$) produces the value $L_d = 13.1 \pm 0.2 \mu\text{m}$ [54]. In a PBC, L_d is even less being a decreasing function of a . To estimate the decrease rate, one can consider the values the mean penetration length L_p of the accepted electrons given in Table I. As in

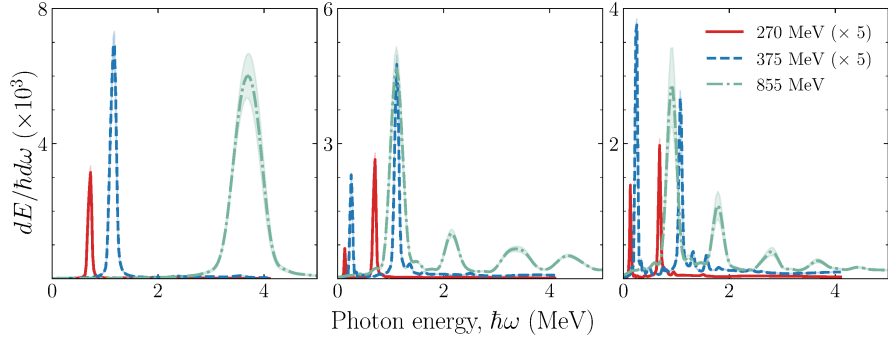


FIG. 3. Emission spectra produced by $\varepsilon = 270, 375$ and 855 MeV positrons in straight (left graph) and PB (middle and right graphs with $a = 2.5$ and 4.0 Å, correspondingly) diamond (110) crystals of thickness $L = 20$ μm . The shaded areas indicate the statistical errors. Note the different scales of the vertical axes.

the positron case, the accepted particles provide the main contribution to the low-energy part of the spectrum dominated by CUR. For higher energies of the emitted radiation, i.e. in the domain of ChR, the contribution of the re-channeled particles to the electron emission spectrum increases. As shown further in the Letter, the dechanneling–re-channeling dynamics together with the strong anharmonicity of the channeling oscillations lead to modifications in the shapes of the electron ChR spectrum different from those discussed for the positrons.

To reveal the evolution of the CUR peak in the electron spectra, one starts with Eq. (1), then follows the arguments outlined above when discussing the positron case, and writes $I_{\text{CUR}}^{(-)}(a) \propto \mathcal{A}(a)L_p(a)a^2$. This relation is adequate when $L_p(a)$ contains at least one CU period. Using the data from Table I for $a = 1.2$ and 2.5 Å, one explains the differences in the CUR intensities in Figs. 1(b) and (d). For $L_p < \lambda_u$, as it occurs for PB with $a = 4$ Å, the radiation becomes more synchrotron-like which manifests itself in broadening of the peak accompanied by additional reduction in its intensity. These features are seen in Fig. 1(d).

The interplay of several processes, occurring in the PBCs, lead to structural transformations in the part of the spectrum $\hbar\omega \gtrsim 2$ MeV

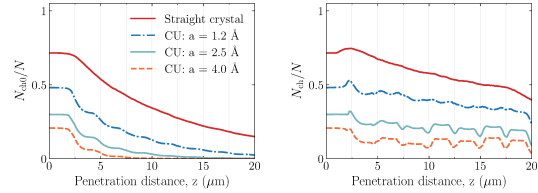


FIG. 4. Fractions of channeling electrons in straight and PB diamond (110) crystals. Left: primary fractions of the accepted particles. Right: fractions with account for the re-channeling. Vertical lines, spaced by the half-period $\lambda_u/2$, mark the points of maximum curvature of the cosine bending profile.

dominated by ChR. This radiation is emitted by all particles experiencing channeling motion. These include the accepted electrons as well as those re-channeled anywhere inside the crystal. It was shown [34] that periodicity in the bending enhances significantly the re-channeling rate even in the limit of large bending curvatures $1/R_{\text{max}}$. As shown, this is in contrast with the dechanneling rate which is virtually equal for both PB and uniformly bent crystalline structures. Left panel in Fig. 4 shows the dependences of the fraction N_{ch0}/N of the accepted electrons which display the channeling motion at the distance z from the entrance. The frac-

tion N_{ch}/N of all electrons (the primarily and the re-channeled ones) that move in the channeling mode are shown on the right panel. The vertical lines mark the points of maximum curvature of the bending profile. At this distances, the effect of de-channeling is the largest leading to the minima of the channeling fraction N_{ch}/N . In contrast, at the distances where the curvature approaches the zero value, the re-channeling yields a significant increase in the number of channeling electrons. The dependence of N_{ch}/N on z allows one to calculate the total length L_{tot} of all channeling segments per a projectile. The corresponding data are presented in the last column of Table I.

For the cosine profile of the bending, electrons enter the PBC in the point of maximum curvature. The centrifugal force filters the particles with respect to the amplitudes a_{ch} , so that similar to the positron case the *accepted* particles oscillate with comparatively small amplitudes. Anharmonicity of the electron channeling oscillations leads to a monotonously decrease of their frequency with a_{ch} . Therefore, the low-frequency channeling oscillations are suppressed. Since the emission frequency is related to Ω_{ch} as $\omega \approx 2\gamma^2\Omega_{\text{ch}}$, one concludes that the ChR spectrum of the accepted particles in PBCs is blue-shifted in comparison with the straight one, and the shift increases with a . This feature is seen in Figs. 1(a)-(d) if one compares the positions of the first maximum (marked with the upward arrow). The account for the emission from the re-channeled electrons allows one to explain why the ChR spectrum does not decrease with a at so high rate as in the positron case. Indeed, re-channeling events occur in the (nearly) straight parts of the PB channel where the centrifugal force is small. Therefore, the amplitude a_{ch} of these particles is uniformly distributed within the interval $a_{\text{ch}} \lesssim d/2$ giving rise to the emission into the whole interval of the ChR energy. As a result, the low-energy part of the ChR is non-zero for all amplitudes considered, and the ratio of the maximum values of the intensity with good

accuracy follows the ratio of the L_{tot} values.

Finally, let us comment on the additional structure (marked with downward arrows) which appears as a hump at ca 10 MeV in Fig. 1(b) and gradually shifts to higher energies as a increases. We attribute it to the coherent BrS radiation which appears in a PBC. In a straight crystal, coherent BrS is emitted by projectiles which traverse the planes under the angle larger than Lindhard's critical angle thus experiencing quasi-regular correlated collisions with the atoms [55]. Its maximum is located well-above that of the ChR (in our case, it is beyond 30 MeV which is the largest abscissa in Fig. 1(a)). Additional, less frequent, periodicity appears in the non-channeling segments of the simulated trajectories in the PBC due to the periodicity in bending. This periodic mode leads to the additional structure in the emitted spectra.

In summary, the channeling and radiation of 855 MeV electrons and positrons in PB diamond (110) crystalline structures has been simulated by means of accurate numerical procedure based on all-atom molecular dynamics. A particular focus of the studies is on the impact of the bending amplitude a on the intensities of the emitted CUR and ChR. We predict, in particular, that for both projectiles the intensity of CUR is a non-monotonous function of a , so that one can find the optimal periodic bending of the crystal planes which ensures the highest yield of CUR. This result is important for the experimental studies of the radiation from CUs as well as for designing and practical realization of PB crystalline structures as the key element of the novel, CU-based light sources. Another important prediction concerns the possibility to manipulate with the ChR intensity by varying the positron beam energy ε and the bending amplitude. In particular, by a proper choice of a one can decrease the ChR intensity by orders of magnitude but, at the same time, maintaining high yield of the CUR. This effect can be utilize to reduce the radiative energy losses which in oriented crystals are mainly due to ChR. Low radiative energy losses maintain the stability of

the CUR signal in thick crystals.

The work was supported in part by the Alexander von Humboldt Foundation Linkage Grant and by the HORIZON 2020 RISE-PEARL project. We acknowledge the Supercomputing Center of Peter the Great Saint-Petersburg Polytechnic University (SPbPU) for providing the opportunities to carry out large-scale simulations. We are grateful to Hartmut Backe and Werner Lauth (University of Mainz) for useful discussions, to Alexey Verkhovtsev (DKFZ) for careful reading of the manuscript and useful comments, and to Alexander Ustinov and Kiril Agapev (SPbPU) for the help in setting the simulations.

* a.pavlov@physics.spbstu.ru

† korol@mbnexplorer.com

- [1] J. Lindhard, K. Dan. Vidensk. Selsk. Mat. Fys. Medd. **34**, 1 (1965).
- [2] M.A. Kumakhov, Phys. Lett. **57A** (1976) 17.
- [3] A.M. Taratin, Phys. Part. Nucl. **29** (1998) 1063.
- [4] A.V. Solov'yov, A. Schäfer, W. Greiner, Phys. Rev. E **53** (1996) 1129.
- [5] H. Shen, Q. Zhao, F.S. Zhang, G.B. Sushko, A.V. Korol, A.V. Solov'yov, Nucl. Instrum. Meth. B **424** (2018) 26.
- [6] A.V. Korol, A.V. Solov'yov, W. Greiner, J. Phys. G **24** (1998) L45.
- [7] A.V. Korol, A.V. Solov'yov, W. Greiner, Int. J. Mod. Phys. E **8** (1999) 49.
- [8] A.V. Korol, A.V. Solov'yov, W. Greiner, *Channeling and Radiation in Periodically Bent Crystals* (Springer-Verlag, Berlin Heidelberg 2014).
- [9] M. Yabashi and H. Tanaka, Nature Photonics **11** (2017) 12.
- [10] W. Greiner, A.V. Korol, A. Kostyuk, A.V. Solov'yov, *Vorrichtung und Verfahren zur Erzeugung elektromagnetischer Strahlung*, Application for German patent, June 14, Ref.: 10 2010 023 632.2 (2010).
- [11] A. Doerr, Nature Meth. **13** (2018) 33.
- [12] E.A. Seddon, J.A. Clarke, D.J. Dunning, C. Masciovecchio, C.J. Milne, F. Parmigiani, D. Rugg, J. C. H. Spence, N.R. Thompson, K. Ueda, S.M. Vinko, J.S. Wark, and W. Wurth, Rep. Prog. Phys. **80** (2017) 115901.
- [13] Ch.J. Milne, Th. Schietinger, M. Aiba, A. Alarcon, J. Alex, A. Anghel, V. Arsov, C. Beard, P. Beaud, S. Bettoni et al., Appl. Sci. **7** (2017) 720.
- [14] P. Emma, R. Akre, J. Arthur, R. Bionta, C. Bostedt, J. Bozek, A. Brachmann, P. Bucksbaum, R. Coffee, F.-J. Decker et al., Nature Photonics **4** (2010) 641.
- [15] B.W.J. McNeil and N.R. Thompson, Nature Photonics **4** (2010) 814.
- [16] K.W.D. Ledingham, P. McKenna, R.P. Singhal, Science **300** (2003) 1107-1111.
- [17] I.A. Solov'yov, A.V. Korol, A.V. Solov'yov, *Multiscale Modeling of Complex Molecular Structure and Dynamics with MBN Explorer* (Springer International Publishing, 2017).
- [18] R. Hajima, T. Haykawa, N. Kikuzawa, E. Minehara, J. Nucl. Sci. Technol. **45** (2008) 441.
- [19] B.M. Weon, J.H. Je, Y. Hwu, G. Margaritondo, Phys. Rev. Lett. **100** (2008) 217403.
- [20] A.V. Korol, A.V. Solov'yov, W. Greiner, Int. J. Mod. Phys. E **13** (2004) 867-916.
- [21] A.V. Korol, A.V. Solov'yov, W. Greiner, J. Phys. G: Nucl. Part. Phys. **27** (2001) 95-125.
- [22] M. Tabrizi, A.V. Korol, A.V. Solov'yov, W. Greiner, Phys. Rev. Lett. **98** (2007) 164801.
- [23] H. Backe, W. Lauth, T.N. Tran Thi, J. Instrum. (JINST) **13** (2018) C04022.
- [24] U.I. Uggerhøj, T.N. Wistisen, J.L. Hansen, W. Lauth, P. Klag, Eur. Phys. J. D **71** (2017) 124.
- [25] T.N. Wistisen, U.I. Uggerhøj, U. Wienands, T.W. Markiewicz, R.J. Noble, B.C. Benson, T. Smith, E. Bagli, L. Bandiera, G. Germogli, V. Guidi, A. Mazzolari, R. Holtzapple, S. Tucker, Phys. Rev. Acc. Beams **19** (2016) 071001.
- [26] T.N. Wistisen, K.K. Andersen, S. Yilmaz, R. Mikkelsen, J.L. Hansen, U.I. Uggerhøj, W. Lauth, H. Backe, Phys. Rev. Lett. **112** (2014) 254801.
- [27] U.I. Uggerhøj, T.N. Wistisen, Nucl. Instrum. Meth. B **355** (2015) 35-39.
- [28] U. Wienands, T. W. Markiewicz, J. Nelson, R.J. Noble, J.L. Turner, U.I. Uggerhøj, T.N. Wistisen, E. Bagli, L. Bandiera, G. Germogli, V. Guidi, A. Mazzolari, R. Holtzapple, M. Miller, Phys. Rev. Lett. **114** (2015) 074801.
- [29] L. Bandiera, E. Bagli, G. Germogli, V. Guidi, M. Mazzolari, H. Backe, W. Lauth, A. Berra, D. Lietti, M. Prest, D. De Salvador, E. Valazza, V. Tikhomirov, Phys. Rev. Lett. **115**

- (2015) 025504.
- [30] H. Backe, W. Lauth, Nucl. Instrum. Meth. B **355** (2015) 24-29.
- [31] A. Mazzolari, E. Bagli, L. Bandiera, V. Guidi, H. Backe, W. Lauth, V. Tikhomirov, A. Berra, D. Lietti, M. Prest, E. Vallazza, D. De Salvador, Phys. Rev. Lett. **112** (2014) 135503.
- [32] E. Bagli, L. Bandiera, V. Bellucci, A. Berra, R. Camattari, D. De Salvador, G. Germogli, V. Guidi, L. Lanzoni, D. Lietti, A. Mazzolari, M. Prest, V. V. Tikhomirov, E. Vallazza, Eur. Phys. J. C **74** (2014) 3114.
- [33] A. Kostyuk, Phys. Rev. Lett. **110** (2013) 115503.
- [34] A.V. Korol, V.G. Bezchastnov, A.V. Solov'yov, Eur. Phys. J. D **171** (2017) 174.
- [35] A.V. Korol, V.G. Bezchastnov, G.B. Sushko, A.V. Solov'yov, Nucl. Instrum. Meth. B **387** (2016) 41-53.
- [36] G.B. Sushko, A.V. Korol, A.V. Solov'yov, Nucl. Instrum. Meth. B **355** (2015) 39.
- [37] R.G. Polozkov, V.K. Ivanov, G.B. Sushko, A.V. Korol, A.V. Solov'yov, Eur. Phys. J. D **68** (2014) 268.
- [38] G.B. Sushko, V.G. Bezchastnov, A.V. Korol, W. Greiner, A.V. Solov'yov, R.G. Polozkov, V.K. Ivanov, J. Phys.: Conf. Ser. **438**, 012019 (2013).
- [39] G.B. Sushko, A.V. Korol, W. Greiner, A.V. Solov'yov, J. Phys.: Conf. Ser. **438** (2013) 012018.
- [40] H. Backe, W. Lauth, *4th Int. Conf. "Dynamics of Systems on the Nanoscale"* (Bad Ems, Germany, Oct. 3-7 2016) Book of Abstracts, p. 58.
- [41] D. Boshoff, M. Copeland, F. Haffeejee, Q. Kilbourn, C. Mercer, A. Osatov, C. Williamson, P. Sihoyiya, M. Motsoai, C.A. Henning, S.H. Connell, T. Brooks, J. Härtwig, T.-N. Tran Thi, N. Palmer, U. Uggerhøj, *4th Int. Conf. "Dynamics of Systems on the Nanoscale"* (Bad Ems, Germany, Oct. 3-7 2016) Book of Abstracts, p. 38.
- [42] U. Wienands, *"Channeling 2016 - Charged&Neutral Particles Channeling Phenomena"* (Sirmione del Garda, Italy, Sept. 25-30 2016).
- [43] Thu Nhi Tran Thi, J. Morse, D. Caliste, B. Fernandez, D. Eon, J. Härtwig, C. Barbay, C. Mer-Calfati, N. Tranchant, J.C. Arnault, T.A. Lafforda, J. Baruche, J. Appl. Cryst. **50** (2017) 561-569.
- [44] I.A. Solov'yov, A.V. Yakubovich, P.V. Nikolaev, I. Volkovets, A.V. Solov'yov, J. Comp. Chem. **33** (2012) 2412-2439.
- [45] <http://mbnresearch.com/get-mbn-explorer-software>
- [46] G.B. Sushko, V.G. Bezchastnov, I.A. Solov'yov, A.V. Korol, W. Greiner, A.V. Solov'yov, J. Comp. Phys. **252** (2013) 404-418.
- [47] V.G. Bezchastnov, A.V. Korol, A.V. Solov'yov, J. Phys. B **47**, 195401 (2014).
- [48] H. Backe, J. Instrum. (JINST) **13** (2018) C02046.
- [49] H. Backe, D. Krambrich, W. Lauth, B. Buonomo, S.B. Dabagov G. Mazzitelli, L. Quintieri, J. Lundsgaard Hansen, U.K.I. Uggerhøj, B. Azadegan, A. Dizdar, W. Wagner, Nuovo Cim. C **34** (2011) 175-180.
- [50] W. Lauth, H. Backe, R. Barret, T.N. Tran Caliste, J. Härtwig, D. Eon, *4th Int. Conf. "Dynamics of Systems on the Nanoscale"* (Bad Ems, Germany, Oct. 3-7 2016) Book of Abstracts, p. 63.
- [51] J. Bak, J.A. Ellison, B. Marsh, F.E. Meyer, O. Pedersen, J.B.B. Petersen, E. Uggerhøj, K. Østergaard, S.P. Møller, A.H. Sørensen, M. Suffert, Nucl. Phys. B **254** (1985) 491-527.
- [52] E.N. Tsyganov, Fermilab Preprint TM-682 (1976).
- [53] V.M. Biryukov, Yu.A. Chesnokov, V.I. Kotov, *Crystal Channeling and its Application at High-Energy Accelerators* (Springer, Berlin, Heidelberg, 1996).
- [54] This result is somewhat lower than the experimental data $24.6 \pm 7.9 \mu\text{m}$ of Backe *et al.* [23]. This difference, however, does not affect the arguments presented in our Letter concerning the evolution of the emission spectra by electrons.
- [55] A.H. Sørensen, Nucl. Instrum. Methods B **119** (1996) 2-29.